Journal of Cerebral Blood Flow & Metabolism (2011) 31, 580–592

www.jcbfm.com

Distinct spatiotemporal patterns of spreading depolarizations during early infarct evolution: evidence from real-time imaging

Tetsuya Kumagai[1,2], Maureen Walberer[1,3], Hajime Nakamura[1,2], Heike Endepols[1], Michael Sué[1], Stefan Vollmar[1], Sasan Adib[1], Günter Mies[1], Toshiki Yoshimine[2], Michael Schroeter[1,3] and Rudolf Graf[1]

[1]*Max Planck Institute for Neurological Research, Cologne, Germany;* [2]*Department of Neurosurgery, Osaka University Graduate School of Medicine, Osaka, Japan;* [3]*Department of Neurology, University Hospital of Cologne, Cologne, Germany*

Experimental and clinical studies indicate that waves of cortical spreading depolarization (CSD) appearing in the ischemic penumbra contribute to secondary lesion growth. We used an embolic stroke model that enabled us to investigate inverse coupling of blood flow by laser speckle imaging (CBF_{LSF}) to CSD as a contributing factor to lesion growth already in the early phase after arterial occlusion. Embolization by macrospheres injected into the left carotid artery of anesthetized rats reduced CBF_{LSF} in the territories of the middle cerebral artery (MCA) (8/14 animals), the posterior cerebral artery (PCA) (2/14) or in less clearly defined regions (4/14). Analysis of MCA occlusions (MCAOs) revealed a first CSD wave starting off during ischemic decline at the emerging core region, propagating concentrically over large portions of left cortex. Subsequent recurrent waves of CSD did not propagate concentrically but preferentially circled around the ischemic core. In the vicinity of the core region, CSDs were coupled to waves of predominantly vasoconstrictive CBF_{LSF} responses, resulting in further decline of *CBF* in the entire inner penumbra and in expansion of the ischemic core. We conclude that CSDs and corresponding *CBF* responses follow a defined spatiotemporal order, and contribute to early evolution of ischemic territories.
Journal of Cerebral Blood Flow & Metabolism (2011) **31,** 580–592; doi:10.1038/jcbfm.2010.128; published online 11 August 2010

Keywords: embolic stroke; experimental; focal brain ischemia; laser speckle imaging; spreading depression

Introduction

Propagating waves of depolarization typically referred to as cortical spreading depression (Leao, 1944*a*) or cortical spreading depolarization (CSD) emerge spontaneously in areas of cerebral cortex surrounding newly developing brain infarcts in animal models of focal ischemia (Hossmann, 1996; Nedergaard and Astrup, 1986), brain trauma (Nilsson *et al*, 1993; Ozawa *et al*, 1991), and subarachnoid hemorrhage (Dreier *et al*, 1998). Moreover, recent clinical studies show that CSD or CSD-like events appear around the site of brain injuries in human patients suffering from acute brain trauma (Strong *et al*, 2002), intracerebral or subarachnoid hemorrhage (Dreier *et al*, 2006; Fabricius *et al*, 2006), and malignant hemispheric stroke (Dohmen *et al*, 2008). These events, alternatively termed peri-infarct depolarization (PID), augment the mismatch between supplied substrate and energy demand of tissue at risk (Busch *et al*, 1996; Takano *et al*, 1996). The number of depolarizations or their cumulative duration is associated with infarct growth (Back *et al*, 1996; Dijkhuizen *et al*, 1999; Mies *et al*, 1993).

A mechanism repeatedly proposed in recent literature as contributing to the devastating effect of CSD in areas around the site of brain injuries is the association of reductions in regional cerebral blood flow (*CBF*) with the depolarizations. This decreased *CBF* has been found in models of subarachnoid hemorrhage (Dreier *et al*, 1998) and focal ischemia (Shin *et al*, 2006; Strong *et al*, 2007), and new evidence exists that they may cause secondary ischemic damage in human brains after subarachnoid hemorrhage (Dreier *et al*, 2009; Iadecola, 2009). In the normally perfused brain, in contrast, *CBF* increases in response to CSD as already shown by Leao (1944*b*) in the second of his two memorable articles.

Of considerable interest for the estimation of CSD contribution to infarct growth is the spatiotemporal

Correspondence: Dr R Graf, Max Planck Institute for Neurological Research, Gleueler Straße 50, 50931 Cologne, Germany.
E-mail: rudolf.graf@nf.mpg.de
Received 3 April 2010; revised 19 June 2010; accepted 13 July 2010; published online 11 August 2010

aspect of the spread of both the depolarization wave and the coupled *CBF* response to this wave, in particular because this response may be inverted (Dunn *et al*, 2001; Shin *et al*, 2006; Strong *et al*, 2007). One unsolved problem is for instance whether CSD and *CBF* responses coupled to CSD participate in the evolution of ischemic territories already in the early phase of occlusive stroke. To address this question, we used real-time imaging with laser speckle flowmetry (*LSF*) covering the dorsolateral aspect of the cortical surface of one hemisphere. The *LSF* has been proved a surrogate tracker of depolarization waves in earlier work (Dunn *et al*, 2001; Shin *et al*, 2006; Strong *et al*, 2007) and is a semiquantitative but fast measure of dynamic CBF_{LSF} alterations. A modified embolic focal ischemia model in rats generated by intracarotid injection of a macrosphere (Gerriets *et al*, 2004) allowed remote occlusion and was therefore especially well suited for continuous imaging during the occlusive process.

Materials and methods

Surgical Preparation

All animal procedures were performed in accordance with the German regulations for animal protection and were approved by the local animal care committee and local governmental authorities. Male Wistar rats ($n = 14$) weighing 300 to 360 g were anesthetized with 5% isoflurane and maintained with 2% to 2.5% isoflurane in a gas mixture of 65% nitrous oxide and 35% oxygen. Throughout the surgical procedures and the experiments, rectal temperature was maintained at 37.5°C, with a thermostatically controlled heating pad. The left femoral artery and vein were cannulated to allow continuous monitoring of arterial blood pressure and intermittent injection of drugs as indicated below. To prepare embolization by a macrosphere, a catheter (PE-50) was inserted into the internal carotid artery (ICA) as described elsewhere (Gerriets *et al*, 2004). In brief, after exposure of the left common carotid artery, ICA, and external carotid artery, the external carotid artery and the pterygopalatine branch of the ICA were ligated. PE-50 tubing filled with heparinized saline and one TiO_2 macrosphere (∅ 0.315 to 0.355 mm; BRACE, Alzenau, Germany) was advanced into the ICA up to the A. pterygopalatine and fixed tightly.

Animals were tracheotomized. After pancuronium injection (first bolus 0.6 mg, followed by 0.4 mg/h), artificial ventilation was started and controlled based on blood gas analysis. The left frontal, parietal, and temporal bones of the rat were exposed and thinned out using a dental drill until they were transparent enough to detect the dura mater (Figure 1A). Drilling was performed under continuous saline irrigation to avoid heat injury. The cavity formed yielded a field of view ($12 \times 7\,mm^2$) that covered a large portion of the dorsolateral cerebral cortex. Paraffin oil was poured into the cavity, and this pool was temperature controlled at 37.0°C using a servo-controlled electrical heating element. Most of the field of view was covered by the territory of the middle cerebral artery (MCA) as confirmed by anatomical studies using post mortem intraarterial Japan ink injection (Figure 1B) in a separate series of experiments not reported here any further.

Laser Speckle Flowmetry

Real-time measurement of CBF_{LSF} has been implemented to study CSD propagation and CSD-associated *CBF* alterations under normal conditions (Ayata *et al*, 2004; Hashemi *et al*, 2009) and in border zones of experimental focal ischemia (Ayata *et al*, 2004; Hashemi *et al*, 2009; Shin *et al*, 2006; Strong *et al*, 2007). Methodological details have been described, and quantification aspects have been discussed (Dunn *et al*, 2001; Strong *et al*, 2006, 2007). In brief, the exposed cortex was illuminated through thinned skull and dura mater with a laser light (laser diode: DL7140-201, 785 nm, 70 mW, Sanyo and laser diode controller: LDC 205B, THORLABS, Newton, NJ, USA) to produce a speckle pattern that was detected with a CCD camera (A602f-2 BASLER, Ahrensburg, Germany). Raw speckle images were acquired with Speckle Contrast Imaging Software (Andrew Dunn, University of Texas at Austin), and speckle contrast images were acquired at a rate of 40 frames/min. To show that CBF_{LSF} is a suitable surrogate marker for CSD, *LSF* measurements were combined with DC recordings in one animal. The bone in one small spot was removed and an Ag/AgCl electrode was positioned on the exposed dura. The DC potential was recorded with a sampling rate of 250 Hz, whereas CBF_{LSF} was measured in a single region of interest (ROI) near the electrode, showing coincidence of the electrical and *CBF* alteration (Figure 1F).

Experimental Design

The *LSF* system (see above) was positioned over the field of view. After collecting baseline images over a period of 5 minutes, ischemia was induced by slow intracarotid injection of a TiO_2 sphere in ~0.2 mL saline and *LSF* was continued for 3 hours. Visual control of *LSF* videos allowed differentiation between various types of territorial ischemic transformation depending on embolization in different cerebral arteries as confirmed by post mortem inspection (Figure 1D). The most common type of occlusion was that of the MCA (8/14 animals; see Table 1). As the MCA territory is well represented in the field of view while others are not (Figure 1B), detailed analysis including statistics was restricted to this entity of eight experimental animals. Mean arterial blood pressure, rectal temperature, and the temperature of the paraffin oil pool were continuously monitored and recorded by a data acquisition system (DASY Lab Ver.9, measX, Mönchengladbach, Germany). Blood gases (pH, pCO_2, PO_2) and blood glucose were only assessed before start and after finishing *LSF* recording to avoid artifactual *LSF* imaging. Experiments were terminated by KCl injection (3 mol/L, 1 mL) immediately after these measurements. In nine animals, isoflurane anesthesia (1.5%) was continued throughout the experiments, in five animals, anesthesia was changed to α-chloralose (80 mg/kg/15 min as a bolus injection and 40 mg/kg/h as a subsequent continuous

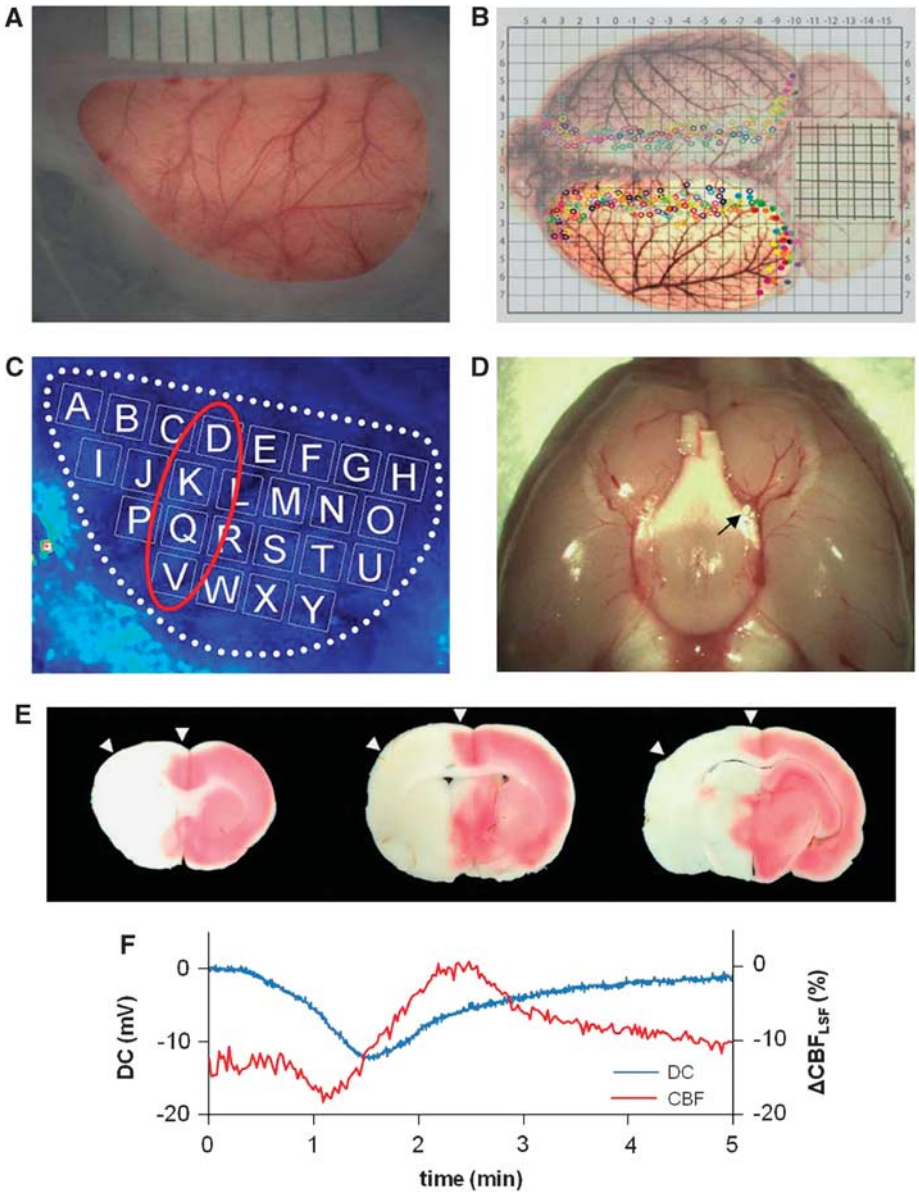

Figure 1 Laser speckle flowmetry (*LSF*) imaging and 'macrosphere' model. (**A**) Photo of field of view (around $12 \times 7\ mm^2$) after thinning the left frontal, parietal, and temporal bones. The cortex can be seen through thinned bone and intact dura mater. (**B**) Distribution of cerebral arteries and artery-to-artery anastomoses shown after transcardial perfusion and staining with Latex/black ink is shown. The cortex in the field of view used for *LSF* imaging was mainly supplied by the left middle cerebral artery (MCA). Many collateral branches from the anterior and posterior cerebral arteries are marked by filled or open circles (colors depict individual animals). (**C**) Speckle contrast image including 25 regions of interest (ROIs) (A–Y), which were used for regional analysis. (**D**) Post mortem view of the base of the brain showing the position of a macrosphere (white particle, see black arrow) at the bifurcation of MCA and anterior cerebral artery (ACA) blocking the anterograde blood flow into the MCA. (**E**) Triphenyltetrazolium chloride (TTC)-stained brain sections showing infarction 1 day after embolization of the MCA that was caused by injection of one macrosphere. These sections confirm that arterial occlusion with one macrosphere has the potential to induce a large infarction. Please note that the example shows a large, almost hemispheric infarction, and does not derive from the analyzed experiments, which were terminated 3 hours after macrosphere injection. Arrowheads indicate that the field of view covered mainly the ischemic penumbra and only part of the core region of the MCA territory. (**F**) Example of the coincidence of DC shift and cerebral blood flow (*CBF*) alteration caused by spreading depolarization occurring spontaneously after injection of a macrosphere and subsequent occlusion of the MCA.

injection) 1 hour before macrosphere injection. In two cases (see Table 1), the experiment was terminated after a shorter period because blood pressure declined suddenly below 70 mmHg. After measurements, the site where the macrosphere was trapped was confirmed by dissection (Figure 1D).

Data Analysis

Image files and video movie files were generated by reconstruction of speckle contrast images using VINCI imaging software (Volume Imaging in Neurological Research, Max Planck Institute for Neurological Research,

Table 1 Summary of results obtained in 14 rats after single macrosphere injection

Animal number	*Observation time (hours)*	*Ischemic territory in field of view*	*Post mortem site of macrosphere*	*Time point of primary wave appearance after macrosphere injection (minutes)*	*Total number of CSDs*	*Mean velocity of CSDs (mm/min)*
1	3	MCAO	MCA (MCA/ACA bifurcation)	2	11	3.11
2	3	Unclear[a]	ICA	5	4	3.88
3	3	MCAO	MCA (MCA/ACA bifurcation)	18	5	3.22
4	3	MCAO	MCA (MCA/ACA bifurcation)	6	5	2.74
5	3	Multiple lesion	ICA	Unclear[b]	Unclear[b]	—
6	3	Unclear[a]	ACA	2	3	3.71
7	3	PCAO	ICA	2	13	3.38
8	3	MCAO	MCA (MCA/ACA bifurcation)	2	7	4.44
9	3	MCAO	MCA (MCA/ACA bifurcation)	1	14	3.75
10	1.4	MCAO	MCA (MCA/ACA bifurcation)	2	4	3.9
11	3	MCAO	MCA (MCA/ACA bifurcation)	1	8	3.84
12	3	MCAO	MCA (MCA/ACA bifurcation)	1	11	3.47
13	3	Multiple lesion	ICA	Unclear[b]	Unclear[b]	—
14	1	PCAO	ICA	8	2	3.61
Mean				4.2	8.1[c]	3.56 ± 0.96

ACA, anterior cerebral artery; CBF, cerebral blood flow; CSD, cortical spreading depolarization; ICA, internal carotid artery; MCAO, middle cerebral artery occlusion; PCA, posterior cerebral artery; PCAO, posterior cerebral artery occlusion; PCOA, posterior communicating artery.

[a]Injection of macrosphere caused CBF reduction, which did not remain consistent throughout the observation period. CBF_{LSF} waves appeared in the field of view.

[b]Ischemic lesions after macrosphere injection were not homogeneous. CBF_{LSF} waves were observed in the field of view but not clearly confined.

[c]Mean of 10 animals observed for 3 hours.

Cologne, Germany). To investigate the spatial and temporal patterns of CSD and associated CBF_{LSF} changes, 25 ROIs ($1.2 \times 1.2\,mm^2$) were equally distributed over the cortical field of view labeled A–Y (Figure 1C). Percent changes of *CBF* were calculated by taking control values averaged over 1.5 minutes before injection of macrospheres as 0% and final values after kill (complete ischemia) as −100%.

Nevertheless, one should take the magnitude of relative flow changes with caution, because factors like unequal thinning of the skull or depth of oil pool have not been corrected for.

Statistics

To test whether MCA occlusion (MCAO) would result in a significant *CBF* reduction, *CBF* values for all ROIs (A–Y) at the time points 1, 2, and 3 hours were tested against preischemic control using the one-sample *t*-test. Resulting *P* values were corrected for multiple comparisons (25 ROIs × 3 time points = 75 tests) using the Benjamini–Hochberg false discovery rate procedure (Benjamini and Hochberg, 1995). $\alpha = 0.05$ was used as significance level in all tests. To test whether development of *CBF* after 3 hours is influenced by initial *CBF* reduction, a linear regression analysis was performed with *CBF* reduction during the first hour as independent variable, and *CBF* reduction after 3 hours as dependent variable.

To investigate the influence of space and time on *CBF* reduction, *CBF* data of all ROIs (A–Y) at all time points (baseline, 5 minutes, 1 hour, 2 hours, and 3 hours) were compared using a two-way repeated measures analysis of variance (ANOVA), with the arc sine square root-transformed data. As tests for normality (Kolmogorov–Smirnov test) and equal variance (Levene median test) failed, a rank transformation was performed before ANOVA. This procedure is suitable for tests of main effects, but inappropriate for testing interactions (Seaman *et al*, 1994). Another ANOVA was therefore calculated with the original data, where interaction of the factors 'ROI' and 'time' was not statistically significant ($F(96;576) = 1.021$; $P = 0.433$). As variance heterogeneity results in an underestimation of type I error, factor interaction was regarded as nonsignificant, and was not tested in the ANOVA on ranks. In the following *post hoc* multiple comparison procedure (Holm–Sidak method), the least affected ROI (A) and the time point 'baseline' were used as controls.

Sorting of ROIs according to baseline *CBF* reduction revealed three groups of high (A–H), middle (I–P), and low (Q–Y) *CBF*. To test whether the groups were significantly different, a one-way ANOVA was performed with the arc sine square root-transformed mean values (across animals) of each ROI (i.e., $n = 8$ for 'high,' $n = 8$ for 'middle,' $n = 9$ for 'low'). Normality and equal variance were tested using the Kolmogorov–Smirnov test and the Levene median test, respectively. ANOVA was followed by an all pairwise

multiple comparison procedure (Holm–Sidak method). A significant difference was detected ($F(2;22) = 337.02$; $P < 0.001$), and *post hoc* comparison revealed that all factor levels (high, middle, and low *CBF*) were significantly different from each other. Subsequently, a two-way repeated measures ANOVA was performed with time (base, 5 minutes (i.e., after passage of the first wave), 1 hour, 2 hours, and 3 hours) used as factor 1, and group (low, middle, and high *CBF*) as factor 2, followed by an all pairwise multiple comparison procedure (Holm–Sidak method).

To evaluate how the development of CBF_{LSF} was influenced by the level of prewave baseline under different conditions (i.e., wave order and height of wave maximum compared with baseline), data were grouped according to four categories: (1) first wave; maximum < base, (2) first wave; maximum > base, (3) subsequent waves; maximum < base, and (4) subsequent waves; maximum > base. Subsequently, linear regression analyses were performed separately for each group, with 'base' as the independent and 'effect' as the dependent variable. To compare the slopes of regression lines, the slope (b) of every data point (base x_i; effect–base y_i) was calculated using the formula

$$b = (x_i - \bar{x})(y_i - \bar{y}),$$

with $\bar{x}$ being the mean of base values, and $\bar{y}$ the mean of effect values. Slopes of the four groups were compared using the Kruskal–Wallis one-way ANOVA on ranks, because data were not normally distributed. *Post hoc* pairwise multiple comparison was performed using Dunn's method.

Results

Already during online CBF_{LSF} imaging, and also retrospectively during analysis of *LSF*-derived videos covering the full-observation period of 3 hours, three principal features of dynamic CBF_{LSF} alterations were observed: (1) a fast, almost immediate gradual decline of CBF_{LSF} after macrosphere injection generating ischemic foci in the arterial territories of the MCA (8/14 animals) or posterior cerebral artery (PCA, 2/14); in other cases (4/14), the attribution to arterial territories was less clear, and eventually, multiple ischemic lesions developed; (2) a primary propagating wave of CBF_{LSF} alteration originating at the border of the ischemic territory soon after the first CBF_{LSF} decline (delay after macrosphere injection: 4.2 minutes) spreading concentrically with a velocity of around 3.4 mm/min and crossing the entire exposed cortex; and (3) multiple subsequent, secondary waves of CBF_{LSF} alteration propagating with similar velocity but taking a circumferential course around the freshly created ischemic territory by avoiding the core region and sometimes regions most distant to the ischemic core. Temporally, secondary waves were distributed almost equally over the 3-hour observation period.

The *CBF* waves turned out to be quite similar to those reported earlier in other models of focal ischemia in lissencephalic brains of mice and gyrencephalic brains of cats (Shin *et al*, 2006; Strong *et al*, 2007). To most easily identify the dynamic nature of the three-mentioned processes, we recommend watching Supplementary Videos 1–4, showing respective three principal features before going into details of the results.

Effects of Embolic Occlusion on CBF_{LSF}

The most frequent effect of macrosphere injection was the immediate evolution of an ischemic lesion in the MCA territory covering a significant portion of the field of view (Table 1; see also Supplementary Video 1). As other types of territorial ischemic transformations were less represented or less clear in their spatial dispersion, forming single or multiple smaller lesions in the field of view (Table 1; see also Supplementary Video 2 displaying the evolution of an ischemic lesion in the territory of the PCA), we restricted formal analysis to occlusions of the MCA. Region of interest analysis of 25 ROIs (Figure 1C) showed gradual decline of CBF_{LSF}, with lowest values in the most lateral and highest values in medial portions of the field of view. ANOVA confirmed that the spatial factor 'ROI' significantly influenced *CBF* reduction ($F(24;576) = 23.24$; $P < 0.001$), and *post hoc* analysis revealed lower CBF_{LSF} values in the three lateral rows of ROIs (I–Y) compared with the medial ROIs (B–H). The gradual decline of CBF_{LSF} is best seen in line plots of mean CBF_{LSF} values taken for individual ROIs over the whole observation period (Figures 2A and 2B) and in sequential stills of videos (Figure 2C). Superimposed waves of CBF_{LSF} appearing repetitively in these line plots document multiple appearance of CSD after MCAO. Interestingly, all ROIs showed a significant decline (one-sample *t*-test against baseline) of mean CBF_{LSF} averaged over the first hour after MCAO (Figures 3A and 3B), even though anterior, medial, and posterior ROIs were not attributable to the MCA territory. This general CBF_{LSF} reduction persisted during the 3-hour observation period (Figure 3C). A weak, even though significant tendency existed for partial recirculation within the 3-hour time frame, being more prominent in ROIs with severe CBF_{LSF} reduction in the MCA territory (Figure 3D, see also Figures 2A and 2B).

Concentric Propagation of First CBF_{LSF} Wave After Middle Cerebral Artery Occlusion

The first CBF_{LSF} wave appeared in most instances very early after arterial occlusion, within or right after the first steep fall of CBF_{LSF} (Table 1). This primary wave was observed in all experiments. It propagated always concentrically, originating from the core of the arising ischemic lesion and crossing the whole field of view. Sequential still images taken from a Laser Speckle video showing the propagation of a primary wave (Figure 4A) illustrate that a front of reduced perfusion

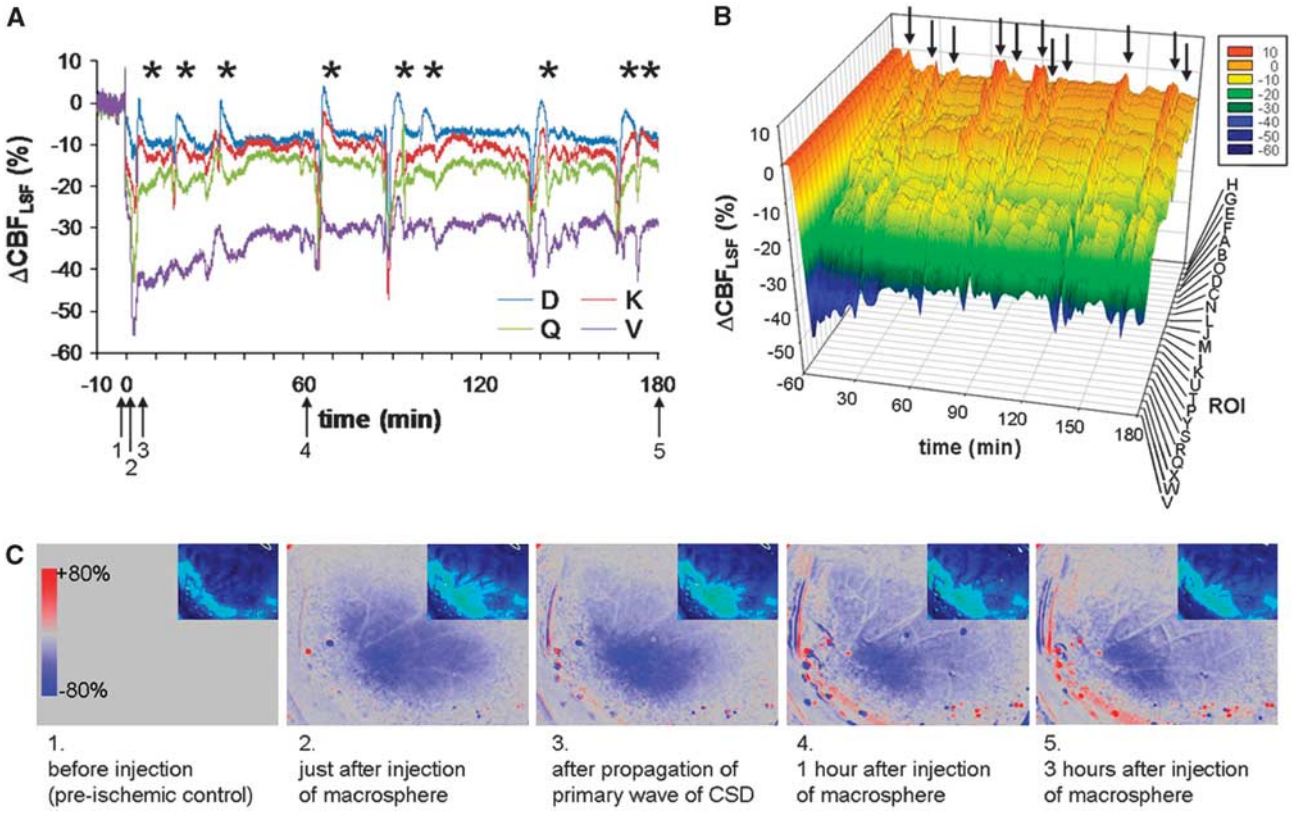

Figure 2 Individual case of CBF_{LSF} changes in individual regions of interest (ROIs) after macrosphere injection. (**A**) Line plots of ΔCBF_{LSF} in selected ROIs. Asterisks indicate CBF_{LSF} waves coupled to cortical spreading depolarizations (CSDs). (**B**) The 3D chart of ΔCBF_{LSF} of all ROIs of the individual animal arranged in order of the initial *CBF* decrease immediately after middle cerebral artery occlusion (MCAO) before appearance of CBF_{LSF} waves. (**C**) Speckle contrast images taken at the time points indicated in Figure 2A by black arrows. In these red and blue images, red signifies hyperemia and blue signifies hypoaemia compared with a baseline image (preinjection image).

(blue) precedes a hyperemic tail of the wave (red). The baseline image taken just before the onset of the first wave ignores the initial reduction of CBF_{LSF} resulting from MCAO to better visualize the effects of the wave (see also Supplementary Video 3). After passage of this first CBF_{LSF} wave, the ischemic lesion appeared intensified as shown by the ischemic transformation superimposed on the primary ischemic focus (region encircled in the last still in Figure 4A by dashed line) and also by the continued decrease of CBF_{LSF} in ROIs in the core-like ROI 'V' (see Figure 4A, line plot). These gradual differences in CBF_{LSF} response patterns become more evident when looking at chart recordings of all 25 ROIs in an individual animal spatially arranged corresponding to ROI arrangement on the cortical surface: monophasic reductions of CBF_{LSF} dominated in core regions (in example presented in Figure 5A, ROIs P–S, V–Y), whereas in border zones of the ischemic focus, biphasic responses (Figure 5A, ROIs A–F, I–O, T–U) or, even more peripherally, monophasic increases of CBF_{LSF} (Figure 5A, ROIs G–H) were characteristic.

Analysis of these response patterns was systematically performed as shown in Figure 6A: separate components of CBF_{LSF} waves (base, minimum, maximum, and effect) were identified for individual waves and related to preischemic control levels of CBF_{LSF}. This analysis revealed that after passage of the primary wave, CBF_{LSF} decreased further in regions with most severe primary ischemia (Figure 6B). In the 'low-*CBF*' group (ROIs Q–Y), CBF_{LSF} was significantly reduced after the passage of the first wave and was still significantly lower than prewave baseline after 3 hours (main effect of factor time: $F(4;88) = 11.5$, $P < 0.0001$; all time points were significantly different from baseline). This secondary CBF_{LSF} reduction was possibly due to lack of a phase of compensatory CBF_{LSF} increase above prewave baseline, reflected by a positive regression between base and effect (see Figure 6C, regression 'maximum < base'). In regions more distant from the core, in contrast, CBF_{LSF} increased after wave passage, indicated by a negative regression between base and effect (see Figure 6C, regression 'maximum > base').

Circumferential Propagation of CBF_{LSF} Waves in the Later Course of Middle Cerebral Artery Occlusion

Subsequent to the primary CBF_{LSF} wave, multiple waves continued to appear over the observation period of 3 hours in all animals with MCAO

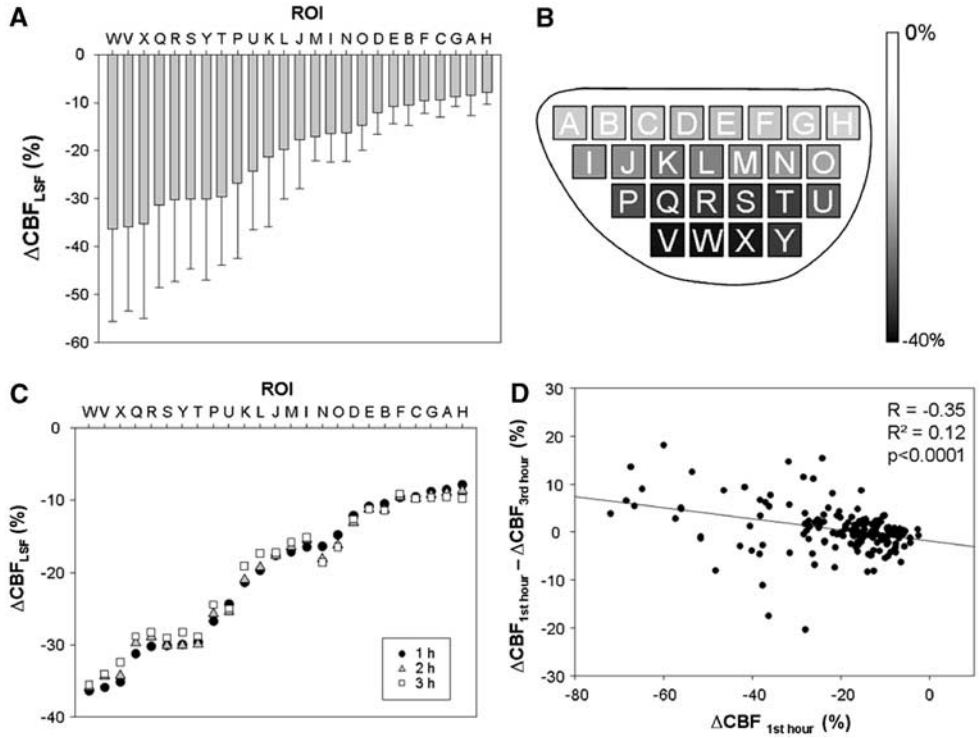

Figure 3 Summary of longitudinal 3-hour region of interest (ROI) analysis of CBF_{LSF} changes after middle cerebral artery occlusion (MCAO) ($n = 7$). (**A**) Mean ΔCBF_{LSF} ($\pm$ s.d.) during first hour after macrosphere injection. In MCAO cases, early ischemic lesion appeared in a concentric manner and ROIs 'W, V, X, Q, R, S, Y, and T' were severely affected. (**B**) Grey level coded representation of mean ΔCBF_{LSF} in respective ROIs during first hour after macrosphere injection. (**C**) Comparison of mean ΔCBF_{LSF} of the first, second, and third 1-hour period in seven MCAO cases. (**D**) The *x* axis is the mean value of ΔCBF_{LSF} of the first hour in all ROIs of seven MCAO animals and the *y* axis is the difference between that of the third hour and the first hour. These show that general CBF_{LSF} reduction persist during the 3-hour observation period (Figure 3C) and weak, even though significant tendency existed for partial recirculation within the 3-hour time frame, being more prominent in ROIs with severe CBF_{LSF} reduction in the MCA territory.

(Table 1). The propagation pattern, however, changed considerably: CBF_{LSF} waves typically came into the field of view from one edge and travelled circumferentially around the freshly developed ischemic core, or they originated near the core propagating then also circumferentially (see Supplementary Video 4). Sequential still images taken from a Laser Speckle video (Figure 4B) illustrate that despite the change in direction of travel, secondary waves resembled the primary waves comprising a front of reduced perfusion (blue) followed by a hyperemic tail of the wave (red). The spatial dispersion of subsequent waves differed insofar as they did not propagate in the ischemic core, if CBF_{LSF} reduction was severe. Therefore, a smaller number of ROIs was crossed by the waves. Further analysis of CBF_{LSF} patterns in circumferential waves revealed spatial differences in proximity to the core: near to the core, monophasic reductions of CBF_{LSF} were dominant (for example as presented in Figure 5B, ROIs P–Q, J–K), whereas with increasing distance to the core, waves became biphasic (Figure 5B, ROIs S–U, I, M–O, A–D) or showed monophasic CBF_{LSF} increases (Figure 5B, ROIs E–H). Thus, response patterns of secondary waves showed a similar, though less pronounced tendency to spatially alter CBF_{LSF} as observed for primary waves: Secondary waves also induced further decreases of CBF_{LSF} in ROIs near the ischemic focus, as indicated by a positive regression between base and effect (see Figure 6D, regression 'maximum < base'). In regions more distant from the core, CBF_{LSF} instead increased after wave passage, as reflected by a negative regression between base and effect (see Figure 6D, regression 'maximum > base'). However, the increase of CBF_{LSF} after secondary waves was less pronounced than after primary waves, leading to a significantly lower slope of the regression line for secondary waves.

Discussion

The central finding in this study was the differentiation between primary and subsequent, secondary waves of cortical blood flow alteration associated with CSD in the area surrounding freshly generated focal ischemic lesions in the 'macrosphere' model of MCAO in rats: primary waves propagated concentrically from the lesion outwards into healthy tissue crossing almost the entire cortex, whereas subsequent waves traveled circumferentially around the

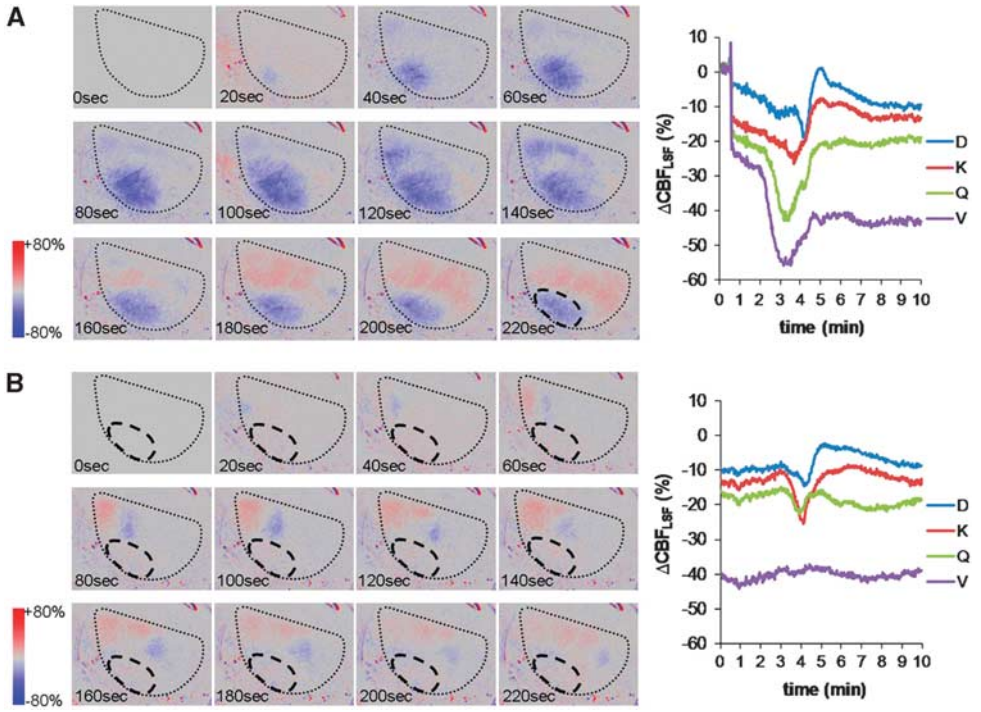

Figure 4 Examples of sequential speckle contrast images of primary concentric and secondary circumferential CBF_{LSF} waves and corresponding line plots of selected region of interest (ROI) analyses. The black dotted line shows the outline of the field of view. The image before initiation of waves (0 second) was chosen as the baseline image. Color coding illustrates increases (red) and decreases of CBF_{LSF} (blue) relative to the baseline image. (**A**) Typical primary CBF_{LSF} wave originating from the lateral edge of the field of view (most ischemic transformation) and propagated concentrically into the periphery of the ischemic territory. The black dashed line in the last image indicates the ischemic lesion remaining after this first wave. The line plot on the right illustrates that in core regions (ROI V, Q), CBF_{LSF} responses to cortical spreading depolarization (CSD) are hypoemic, with additional reduction seen in the most central region (ROI V), whereas regions in the surrounding of the ischemic core are biphasic, with a pronounced hyperemic portion of the response. (**B**) Secondary CBF_{LSF} wave with hypoemic (blue) wave front and a hyperemic (red) wave tail propagating circumferentially along the core of the ischemic territory (black dashed line).

lesion, and the dispersion of secondary waves was more or less restricted to the lesion border. The second finding of relevance relates to the use of *LSF* as a measure of regional blood flow: CBF_{LSF} waves were polymorphic as described for several models of focal ischemia (Luckl *et al*, 2009; Shin *et al*, 2006; Strong *et al*, 2007). Both primary and secondary types of CBF_{LSF} waves contributed to the evolution of the ischemic lesion, the primary having more impact in the observed early phase.

A major benefit of using the 'macrosphere' model in combination with *LSF* was its suitability to remotely occlude a cerebral artery (Gerriets *et al*, 2004) allowing continuous observation in real time: (1) the consequences of macrosphere arrival, (2) the ischemic focus in *status nascendi*, and (3) the immediate onset of multiple CBF_{LSF} wave passages over significant portions of cerebral cortex. The model used did not allow observation of the whole circumference of the lesion as previously shown by our group in a 'distal' MCAO model with coagulation of a distal branch of the MCA that enabled us to observe cyclic repetitive propagation of PID-associated CBF_{LSF} waves around the ischemic focus (Nakamura *et al*, 2010). In the 'distal' MCAO model, however, the transition from preischemic to ischemic conditions was not available, and therefore, a differentiation between primary and secondary waves was impossible.

Laser speckle imaging was introduced in 2001 for the study of *CBF* (Dunn *et al*, 2001), and has been applied since to examine *CBF* alterations related to functional brain activation and spreading depression in physiological conditions (Ayata *et al*, 2004; Dunn *et al*, 2003; Durduran *et al*, 2004; Obrenovitch *et al*, 2009; Sakadzic *et al*, 2009), as well as to focal cerebral ischemia and associated PIDs (Luckl *et al*, 2009; Shin *et al*, 2006, 2007; Strong *et al*, 2007). Despite the fact that quantification may be obtained under optimal experimental conditions (Strong *et al*, 2006), we used *LSF* as a relative measure implementing a scale that took preischemic control values before macrosphere injection as zero, and post mortem values as −100%. Even though the linearity of this scale remains obscure, the data obtained were convincing with regard to the use of *LSF* as a tool to (1) dynamically examine the evolution of an ischemic focus, (2) track CSDs, and (3) distinguish between different patterns of *CBF* transients in response to CSD.

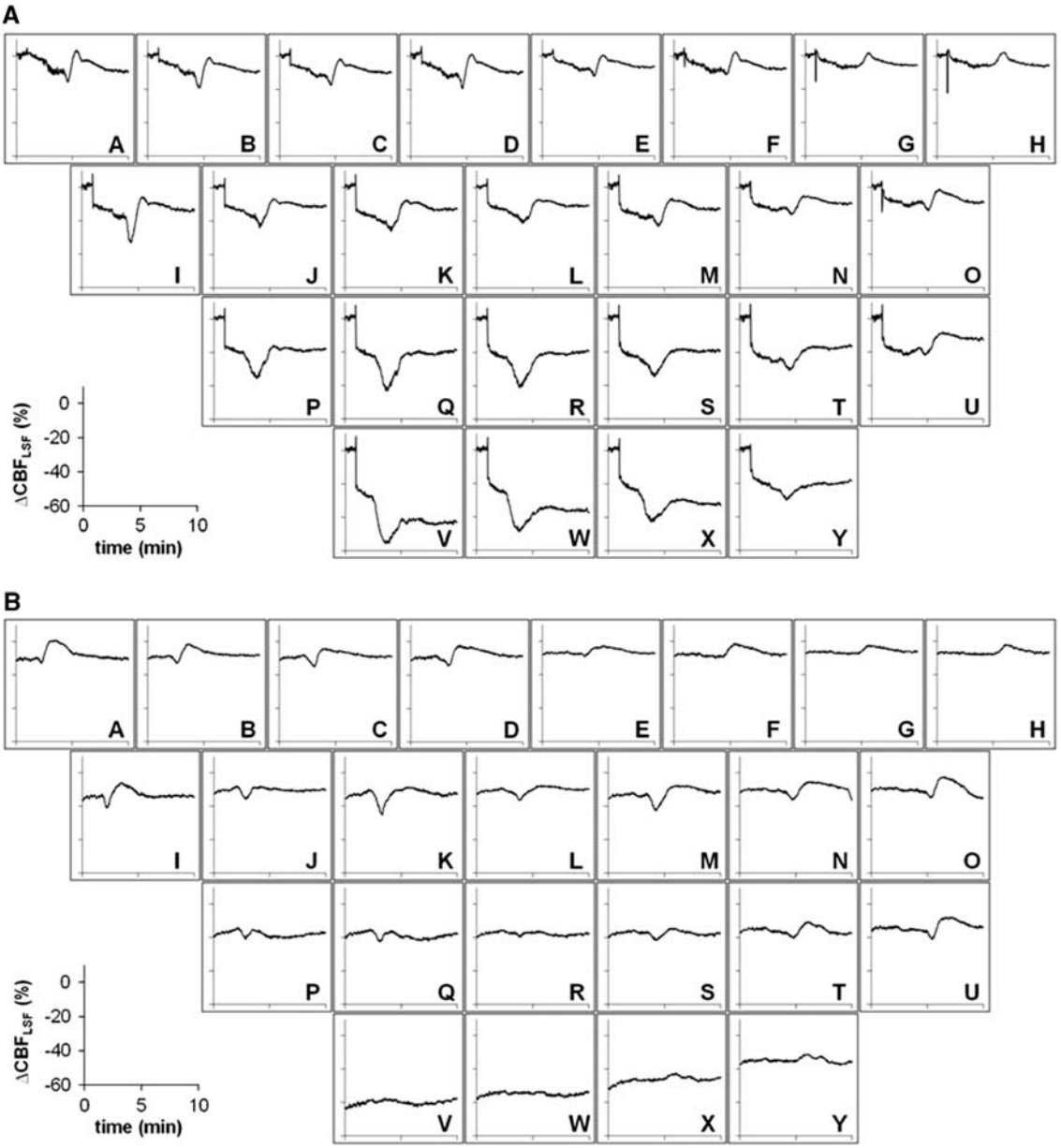

Figure 5 Examples of line plots of a primary concentric and a secondary circumferential CBF_{LSF} wave analyzed over 10 minutes for the whole set of 25 individual regions of interest (ROIs). (**A**) The primary concentric wave appeared in each ROI showing monophasic hypoemic wave morphology in frontolateral ROIs (VWX and PQR) and biphasic or monophasic hyperemic morphology in medial ROIs. (**B**) The secondary circumferential wave showed a similar wave morphology with respect to the *CBF* gradient within the ischemic focus, but CBF_{LSF} waves were not observed in the core of the ischemic territory.

The *LSF* allowed observation of the rapid evolution of ischemic foci: in the eight animals developing a typical spatial pattern of MCAO in our study, the ischemic territory began to form only seconds after the macrosphere got trapped (see Supplementary Video 1). Only in these animals did post mortem analysis reveal that the site of macrosphere trapping was indeed the MCA/anterior cerebral artery (ACA) bifurcation. A rather large portion of animals (6/14) did not develop clear spatial patterns of ischemia. In these animals, macrospheres were mostly trapped in the ICA. The high rate of failure to produce a clear ischemic focus may be regarded disadvantageous and is most probably due to our use of a single rather than four macrospheres, as was the case in former studies using this model (Gerriets *et al*, 2004). The time point of occlusion seemed to us less well defined, with injection of four macrospheres even though the incidence of successful occlusion is presumably higher and infarction larger. In our study, however, we were particularly interested in the temporal relationship between onset of ischemia and appearance of the first wave as compared with subsequent waves of CSD-related

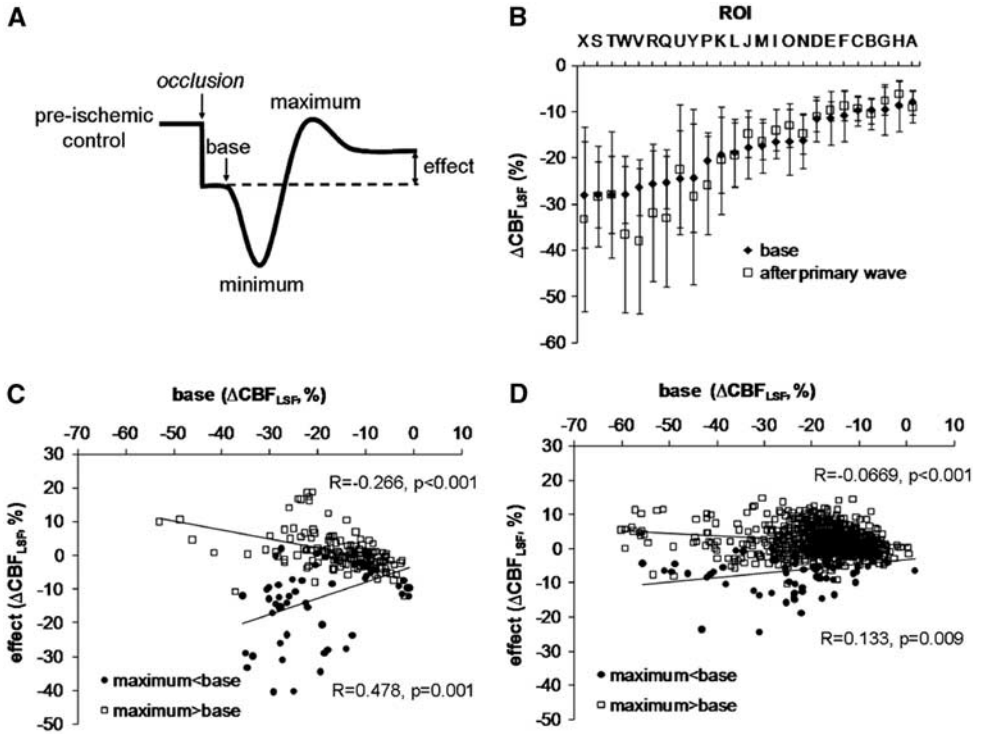

Figure 6 Summary of region of interest (ROI) analysis of cortical spreading depolarization (CSD)-coupled CBF_{LSF} waves ($n = 8$). (**A**) Schema of a (primary) biphasic CBF_{LSF} response, with segments ('base,' 'minimum,' 'maximum,' and 'effect') used to describe and analyze the morphology of the wave. (**B**) Means (± s.d.) of 'base' and 'effect' of primary waves ($n = 7$). After passage of the primary wave, CBF_{LSF} decreased particularly in ROIs with severe primary ischemia. (**C**) Correlation between 'base' and 'effect' analyzed in individual ROIs of primary concentric waves, showing CBF_{LSF} increases (positive, 'compensatory' effects of the waves) in cases with 'maximum' above base level (maximum > base) and CBF_{LSF} decreases (negative effects of the waves) in cases with 'maximum' below base level (maximum < base). (**D**) Correlation between 'base' and 'effect' analyzed in individual ROIs of secondary circumferential waves showing, similar to primary waves but less distinct, CBF_{LSF} increases in cases with 'maximum' above base level (maximum > base) and CBF_{LSF} decreases in cases with 'maximum' below base level (maximum < base).

CBF transients and thus wanted to avoid ambiguity in the temporal generation of the ischemic focus derived from variable time points of occlusion because of sequential trapping of multiple macrospheres in various arterial branches.

Regarding the general effects of MCAO, CBF_{LSF} decreased gradually, the most lateral ROIs showing most severe reductions. It was remarkable that small but consistent decreases of CBF_{LSF} were even observed in medial ROIs attributable to the ACA territory and in occipital ROIs attributable to the PCA territory. This might reflect a condition similar to the 'reversible cerebral vasoconstriction syndrome' described in human patients (Ducros and Bousser, 2009), a general vasoconstriction, which can be caused by mechanical damage to major arteries.

Surprisingly, in most animals including not only those with clear signs of MCAO but also those with ICA or ACA involvement, primary CBF_{LSF} waves developed rapidly within the first few minutes after macrosphere injection appearing in the field of view of the laser speckle system. These waves turned up during or immediately after the first occlusive reduction of *CBF*. In case of MCAO, primary CBF_{LSF} waves always propagated concentrically originating in the most lateral ROIs spreading concentrically in medio–occipito–frontal direction. Waves typically crossed all 25 analyzed ROIs, and we suspect that they spread over the entire cortex. Concentric wave propagation of CSDs has been described in rats and cats under physiological conditions after induction with high potassium (Farkas *et al*, 2008; Smith *et al*, 2001; Tomita *et al*, 2002). In focal ischemia, in contrast, rostral-caudal or circumferential propagation around the ischemic core seems to be the predominant pattern (Hartings *et al*, 2003; Luckl *et al*, 2009; Nakamura *et al*, 2010). Only in one study in cats, was radial propagation from the core to the periphery showed during the early phase after proximal MCAO (Nakamura *et al*, 2010). As concentric propagation seems to be restricted to the initial phase of focal ischemia, tissue conditions might still be quite normal early after occlusion and comparable to the conditions encountered during artificial CSD induction in physiological conditions.

The form of the primary waves was polymorph as described for other models of focal ischemia (Luckl *et al*, 2009; Strong *et al*, 2007; Sukhotinsky *et al*, 2008), but not consistent throughout the course of spread. Rather, waves started as predominantly

monophasic hypoperfusion waves, and as they travelled into the border zone of the ischemic focus, they became biphasic, with a phase of hypoperfusion preceding a hyperemic phase. Thereafter, in the periphery of the focus, they became almost purely hyperemic and thus again monophasic. This transition took place in watershed zones between arterial territories of the MCA on the one side and those of the ACA and PCA on the other. For primary waves, we assume that the transition of morphology is characteristic for their travel through changing conditions into the periphery of the developing focus, and they may therefore represent an excellent model to study underlying mechanisms of normal or inverted coupling of blood flow to spreading depolarization as first described by Dreier *et al* (1998) in a model of subarachnoid hemorrhage. Furthermore, they may indeed participate in the maturation of zonal gradation of ischemic foci: in inner zones near the wave origin exhibiting most severe ischemic reductions of *CBF*, these hemodynamic transients cause a further decline of *CBF* compared with outer zones because of the fact that compensatory hyperemic portions of the transients are missing here while they are pronounced in outer zones. To illustrate this phenomenon, we have separated ROIs with intact compensatory abilities (condition 'maximum > base') from those where compensation is no longer possible (condition 'maximum < base'), and performed separate regression analyses between the variables 'base' (the prewave baseline) and 'effect' (CBF_{LSF} level after passage of the wave) with the two groups (see Figure 6C). The compensatory mechanisms of intact tissue are impressively shown by the negative slope of the regression line in the condition 'maximum > base,' indicating that the lower the initial CBF_{LSF}, the more effective the reperfusion after the first CSD. In contrast, in the group 'maximum < base,' the regression was positive, demonstrating that the lower the initial CBF_{LSF}, the stronger its further decline. As a result, the demarcation between inner and outer zones is enhanced after the passage of primary waves.

In animals developing MCAO, the next CBF_{LSF} waves after primary concentric waves already showed a completely different spatial course of propagation: they travelled around the core region, the main direction being rostral-caudal or reverse, respectively, clockwise or counterclockwise. This spatial pattern of CBF_{LSF} wave propagation remained predominant for subsequent waves throughout the 3-hour observation period. Our finding indicates that under pathophysiological conditions like those developing in the ischemic border zone after arterial occlusion, the basis for propagation of PIDs or CBF_{LSF} waves substantially changes soon after MCAO leading to the change of the spatiotemporal propagation pattern. What are the essential alterations of tissue conditions that may affect the spatiotemporal pattern of spread? Despite substantial efforts, the mechanism of CSD or PID propagation has never been convincingly identified. Two major hypotheses have been proposed, one postulating extracellular mechanisms of diffusion of substances like potassium or glutamate, which are involved in the process of depolarization and appear in rather high extracellular concentrations during CSD, the other suggesting intercellular propagation of substances like potassium through gap junctions, either between neurons or between glial cells (Somjen, 2001). In core regions of evolving ischemic foci, substances like potassium and glutamate are excessively liberated shortly after anoxic depolarization and presumably diffuse into the surrounding border zones (Shimada *et al*, 1989). Thus, if CSD induction occurs at some time point at the edge of the ischemic core, this depolarization will cause additional release of potassium and glutamate and may thereby easily initiate, presumably in a cascade-like manner, depolarization around the whole circumference of an ischemic border zone, where potassium and glutamate concentrations are already elevated by diffusion from the core—a process that takes some time, possibly the time elapsing between first and subsequent waves. We assume that it is this time point that marks the transition of cortical tissue into conditions of the ischemic penumbra. Extracellular potassium transients in particular were reported already in the 1970s to characterize such conditions (Branston *et al*, 1977). The ischemic penumbra, therefore, is perhaps primed or preconditioned for preferential CSD/PID propagation as soon as anoxic depolarization has occurred in the core region resulting in the liberation of substances like potassium and glutamate and diffusion of these substances into this region. As a consequence, rostral-caudal or circumferential propagation around the ischemic core seems to emerge as the predominant pattern of CSD/PID propagation in focal ischemia of cats and rats (Hartings *et al*, 2003; Luckl *et al*, 2009; Nakamura *et al*, 2010). Even more convincingly, we have recently been able to show in rats in a model of occlusion of distal branches of the MCA that CBF_{LSF} waves circle not only once but multiple times around an ischemic lesion that was substantially smaller than in the model used in this study so that the whole circumference of the lesion could be visualized by *LSF* (Nakamura *et al*, 2010). Regarding the dispersion of primary and secondary CBF_{LSF} waves, it is also interesting to note that only primary waves appeared in almost all ROIs covering perhaps the whole hemisphere, whereas secondary CBF_{LSF} waves did not appear in the most lateral ROIs (see Figure 5) representing core regions of the MCAO. It is well known that CSDs do not propagate in injured or infarcted tissue (Somjen, 2001), and therefore we consider ROIs without a secondary wave ischemic core. It seems obvious that not only penumbra but also core conditions evolve spatially in a highly dynamic manner during this early stage of arterial occlusion, and it should be mentioned in this context that other mechanisms like increased oxygen extraction in ischemic border zone regions (Heiss *et al*, 1994) participate in this spatially transitional phase.

With respect to the emergence of a gradual decline in *CBF* in the ischemic territory, secondary CBF_{LSF} waves showed similar polymorphism as that found for primary waves: in the inner penumbra near the ischemic core, monophasic reductions of perfusion were dominant, whereas monophasic increases of *CBF* were seen in most peripheral ROIs. Biphasic responses with decreases followed by increases of *CBF* were mostly observed in the outer penumbra. Similar polymorphism has been documented in other models of focal ischemia in cats and rats (Luckl *et al*, 2009; Shin *et al*, 2006; Strong *et al*, 2007). It seems that in outer zones, anastomoses between arterioles of the ischemic MCA territory and the neighboring ACA and PCA territories work efficiently to allow *CBF* elevation through collateral channels, whereas in inner zones, this type of coupling of *CBF* to depolarization seems to be more and more reversed. As a mechanism of inverted coupling during CSD, nitric oxide synthase inhibition in the presence of raised potassium has been discussed (Dreier *et al*, 1998), indicating that under physiological conditions, nitric oxide mediates increases of cerebral perfusion coupled to CSD. Even though the effect of secondary CBF_{LSF} waves on a further reduction of *CBF* in inner zones of the penumbra seems rather small from our results (see Figure 6), it should be emphasized that multiple CSDs/PIDs are to be expected in the course of focal ischemia and stroke resulting in additive deleterious effects, in particular, if clusters of CSD/PID appear (Bosche *et al*, 2010; Dohmen *et al*, 2008; Dreier *et al*, 2006). In SAH patients, for example, we have recently shown that within clusters of CSD, oxygen availability decreases considerably (Bosche *et al*, 2010; Dohmen *et al*, 2008; Dreier *et al*, 2006). Similarly, extracellular glucose availability may decrease after CSD passage, which even occurs under almost physiological conditions (Hashemi *et al*, 2009).

We conclude that the primary CSD or CBF_{LSF} wave after an ischemic stroke is most relevant in terms of initially separating tissue compartments where compensatory mechanisms are still possible from those where *CBF* reduction can no longer be compensated. In contrast to the primary wave, which travels across the whole hemisphere, the secondary waves mostly remain in the ischemic border zone and contribute to its differentiation. The CSDs therefore seem to act as a trigger mechanism of infarct evolution.

Disclosure/conflict of interest

The authors declare no conflict of interest.

References

Ayata C, Shin HK, Salomone S, Ozdemir-Gursoy Y, Boas DA, Dunn AK, Moskowitz MA (2004) Pronounced hypoperfusion during spreading depression in mouse cortex. *J Cereb Blood Flow Metab* 24:1172–82

Back T, Ginsberg MD, Dietrich WD, Watson BD (1996) Induction of spreading depression in the ischemic hemisphere following experimental middle cerebral artery occlusion: effect on infarct morphology. *J Cereb Blood Flow Metab* 16:202–13

Benjamini Y, Hochberg Y (1995) Controlling the false discovery rate: a practical and powerful approach to multiple testing. *J Roy Statist Soc Ser B* 57:289–300

Bosche B, Graf R, Ernestus RI, Dohmen C, Reithmeier T, Brinker G, Strong AJ, Dreier JP, Woitzik J (2010) Recurrent spreading depolarizations after SAH decrease oxygen availability in human cerebral cortex. *Ann Neurol* 67:607–17

Branston NM, Strong AJ, Symon L (1977) Extracellular potassium activity, evoked potential and tissue blood flow. Relationships during progressive ischaemia in baboon cerebral cortex. *J Neurol Sci* 32:305–21

Busch E, Gyngell ML, Eis M, Hoehn-Berlage M, Hossmann KA (1996) Potassium-induced cortical spreading depressions during focal cerebral ischemia in rats: contribution to lesion growth assessed by diffusion-weighted NMR and biochemical imaging. *J Cereb Blood Flow Metab* 16:1090–9

Dijkhuizen RM, Beekwilder JP, van der Worp HB, Berkelbach van der Sprenkel JW, Tulleken KA, Nicolay K (1999) Correlation between tissue depolarizations and damage in focal ischemic rat brain. *Brain Res* 840:194–205

Dohmen C, Sakowitz OW, Fabricius M, Bosche B, Reithmeier T, Ernestus RI, Brinker G, Dreier JP, Woitzik J, Strong AJ, Graf R (2008) Spreading depolarizations occur in human ischemic stroke with high incidence. *Ann Neurol* 63:720–8

Dreier JP, Korner K, Ebert N, Gorner A, Rubin I, Back T, Lindauer U, Wolf T, Villringer A, Einhaupl KM, Lauritzen M, Dirnagl U (1998) Nitric oxide scavenging by hemoglobin or nitric oxide synthase inhibition by N-nitro-L-arginine induces cortical spreading ischemia when K+ is increased in the subarachnoid space. *J Cereb Blood Flow Metab* 18:978–90

Dreier JP, Major S, Manning A, Woitzik J, Drenckhahn C, Steinbrink J, Tolias C, Oliveira-Ferreira AI, Fabricius M, Hartings JA, Vajkoczy P, Lauritzen M, Dirnagl U, Bohner G, Strong AJ (2009) Cortical spreading ischaemia is a novel process involved in ischaemic damage in patients with aneurysmal subarachnoid haemorrhage. *Brain* 132:1866–81

Dreier JP, Woitzik J, Fabricius M, Bhatia R, Major S, Drenckhahn C, Lehmann TN, Sarrafzadeh A, Willumsen L, Hartings JA, Sakowitz OW, Seemann JH, Thieme A, Lauritzen M, Strong AJ (2006) Delayed ischaemic neurological deficits after subarachnoid haemorrhage are associated with clusters of spreading depolarizations. *Brain* 129:3224–37

Ducros A, Bousser MG (2009) Reversible cerebral vasoconstriction syndrome. *Pract Neurol* 9:256–67

Dunn AK, Bolay H, Moskowitz MA, Boas DA (2001) Dynamic imaging of cerebral blood flow using laser speckle. *J Cereb Blood Flow Metab* 21:195–201

Dunn AK, Devor A, Bolay H, Andermann ML, Moskowitz MA, Dale AM, Boas DA (2003) Simultaneous imaging of total cerebral hemoglobin concentration, oxygenation, and blood flow during functional activation. *Opt Lett* 28:28–30

Durduran T, Burnett MG, Yu G, Zhou C, Furuya D, Yodh AG, Detre JA, Greenberg JH (2004) Spatiotemporal quantification of cerebral blood flow during functional

activation in rat somatosensory cortex using laser-speckle flowmetry. *J Cereb Blood Flow Metab* 24:518–25
Fabricius M, Fuhr S, Bhatia R, Boutelle M, Hashemi P, Strong AJ, Lauritzen M (2006) Cortical spreading depression and peri-infarct depolarization in acutely injured human cerebral cortex. *Brain* 129:778–90
Farkas E, Pratt R, Sengpiel F, Obrenovitch TP (2008) Direct, live imaging of cortical spreading depression and anoxic depolarisation using a fluorescent, voltage-sensitive dye. *J Cereb Blood Flow Metab* 28:251–62
Gerriets T, Stolz E, Walberer M, Muller C, Kluge A, Kaps M, Fisher M, Bachmann G (2004) Middle cerebral artery occlusion during MR-imaging: investigation of the hyperacute phase of stroke using a new in-bore occlusion model in rats. *Brain Res Brain Res Protoc* 12:137–43
Hartings JA, Rolli ML, Lu XC, Tortella FC (2003) Delayed secondary phase of peri-infarct depolarizations after focal cerebral ischemia: relation to infarct growth and neuroprotection. *J Neurosci* 23:11602–10
Hashemi P, Bhatia R, Nakamura H, Dreier JP, Graf R, Strong AJ, Boutelle MG (2009) Persisting depletion of brain glucose following cortical spreading depression, despite apparent hyperaemia: evidence for risk of an adverse effect of Leao's spreading depression. *J Cereb Blood Flow Metab* 29:166–75
Heiss WD, Graf R, Wienhard K, Lottgen J, Saito R, Fujita T, Rosner G, Wagner R (1994) Dynamic penumbra demonstrated by sequential multitracer PET after middle cerebral artery occlusion in cats. *J Cereb Blood Flow Metab* 14:892–902
Hossmann KA (1996) Periinfarct depolarizations. *Cerebrovasc Brain Metab Rev* 8:195–208
Iadecola C (2009) Bleeding in the brain: killer waves of depolarization in subarachnoid bleed. *Nat Med* 15: 1131–2
Leao AAP (1944*a*) Spreading depression of activity in the cerebral cortex. *J Neurophysiol* 7:359–90
Leao AAP (1944*b*) Pial circulation and spreading depression of activity in cerebral cortex. *J Neurophysiol* 7:391–6
Luckl J, Zhou C, Durduran T, Yodh AG, Greenberg JH (2009) Characterization of periinfarct flow transients with laser speckle and Doppler after middle cerebral artery occlusion in the rat. *J Neurosci Res* 87:1219–29
Mies G, Iijima T, Hossmann KA (1993) Correlation between peri-infarct DC shifts and ischaemic neuronal damage in rat. *Neuroreport* 4:709–11
Nakamura H, Strong AJ, Dohmen C, Sakowitz OW, Vollmar S, Sue M, Kracht L, Hashemi P, Bhatia R, Yoshimine T, Dreier JP, Dunn AK, Graf R (2010) Spreading depolarizations cycle around and enlarge focal ischaemic brain lesions. *Brain* 133(Pt 7):1994–2006
Nedergaard M, Astrup J (1986) Infarct rim: effect of hyperglycemia on direct current potential and [14C]2-deoxyglucose phosphorylation. *J Cereb Blood Flow Metab* 6:607–15
Nilsson P, Hillered L, Olsson Y, Sheardown MJ, Hansen AJ (1993) Regional changes in interstitial K+ and Ca2+ levels following cortical compression contusion trauma in rats. *J Cereb Blood Flow Metab* 13:183–92
Obrenovitch TP, Chen S, Farkas E (2009) Simultaneous, live imaging of cortical spreading depression and associated cerebral blood flow changes, by combining voltage-sensitive dye and laser speckle contrast methods. *NeuroImage* 45:68–74
Ozawa Y, Nakamura T, Sunami K, Kubota M, Ito C, Murai H, Yamaura A, Makino H (1991) Study of regional cerebral blood flow in experimental head injury: changes following cerebral contusion and during spreading depression. *Neurol Med Chir (Tokyo)* 31:685–90
Sakadzic S, Yuan S, Dilekoz E, Ruvinskaya S, Vinogradov SA, Ayata C, Boas DA (2009) Simultaneous imaging of cerebral partial pressure of oxygen and blood flow during functional activation and cortical spreading depression. *Appl Opt* 48:D169–77
Seaman JW, Walls SC, Wide SE, Jaeger RG (1994) Caveat emptor: rank transform methods and interactions. *Trends Ecol Evol* 9:261–3
Shimada N, Graf R, Rosner G, Wakayama A, George CP, Heiss WD (1989) Ischemic flow threshold for extracellular glutamate increase in cat cortex. *J Cereb Blood Flow Metab* 9:603–6
Shin HK, Dunn AK, Jones PB, Boas DA, Lo EH, Moskowitz MA, Ayata C (2007) Normobaric hyperoxia improves cerebral blood flow and oxygenation, and inhibits peri-infarct depolarizations in experimental focal ischaemia. *Brain* 130:1631–42
Shin HK, Dunn AK, Jones PB, Boas DA, Moskowitz MA, Ayata C (2006) Vasoconstrictive neurovascular coupling during focal ischemic depolarizations. *J Cereb Blood Flow Metab* 26:1018–30
Smith JM, James MF, Bockhorst KH, Smith MI, Bradley DP, Papadakis NG, Carpenter TA, Parsons AA, Leslie RA, Hall LD, Huang CL (2001) Investigation of feline brain anatomy for the detection of cortical spreading depression with magnetic resonance imaging. *J Anat* 198:537–54
Somjen GG (2001) Mechanisms of spreading depression and hypoxic spreading depression-like depolarization. *Physiol Rev* 81:1065–96
Strong AJ, Anderson PJ, Watts HR, Virley DJ, Lloyd A, Irving EA, Nagafuji T, Ninomiya M, Nakamura H, Dunn AK, Graf R (2007) Peri-infarct depolarizations lead to loss of perfusion in ischaemic gyrencephalic cerebral cortex. *Brain* 130:995–1008
Strong AJ, Bezzina EL, Anderson PJ, Boutelle MG, Hopwood SE, Dunn AK (2006) Evaluation of laser speckle flowmetry for imaging cortical perfusion in experimental stroke studies: quantitation of perfusion and detection of peri-infarct depolarisations. *J Cereb Blood Flow Metab* 26:645–53
Strong AJ, Fabricius M, Boutelle MG, Hibbins SJ, Hopwood SE, Jones R, Parkin MC, Lauritzen M (2002) Spreading and synchronous depressions of cortical activity in acutely injured human brain. *Stroke* 33:2738–43
Sukhotinsky I, Dilekoz E, Moskowitz MA, Ayata C (2008) Hypoxia and hypotension transform the blood flow response to cortical spreading depression from hyperemia into hypoperfusion in the rat. *J Cereb Blood Flow Metab* 28:1369–76
Takano K, Latour LL, Formato JE, Carano RA, Helmer KG, Hasegawa Y, Sotak CH, Fisher M (1996) The role of spreading depression in focal ischemia evaluated by diffusion mapping. *Ann Neurol* 39:308–18
Tomita Y, Tomita M, Schiszler I, Amano T, Tanahashi N, Kobari M, Takeda H, Ohtomo M, Fukuuchi Y (2002) Repetitive concentric wave-ring spread of oligemia/hyperemia in the sensorimotor cortex accompanying K(+)-induced spreading depression in rats and cats. *Neurosci Lett* 322:157–60

Supplementary Information accompanies the paper on the Journal of Cerebral Blood Flow & Metabolism website (http://www.nature.com/jcbfm)